Preprints of the 21st IFAC World Congress (Virtual)
Berlin, Germany, July 12-17, 2020

Evaluation of Nonlinear System Identification to Model Piezoacoustic Transmission

Matheus Patrick Soares Barbosa * **Daniel Pereira da Costa** *
Helon Vicente Hultmann Ayala *

* *Dep. of Machanical Engineering, Pontifical Catholic University of Rio de Janeiro, Brazil (e-mails: mpatrick.barbosa@gmail.com, daniel.pereiracosta@hotmail.com, helon@puc-rio.br)*

Abstract: Piezoeletric materials are used on high-precision and high-dynamics applications, such as for acoustic transmission. This paper covers the challenges of creating a black-box model for a simultaneous acoustic transmission problem, with data acquired in a laboratory setup. The system performance is analyzed for three different models: AutoRegressive Moving Average with eXogenous inputs (ARMAX) model, Nonlinear AutoRegressive with eXogenous inputs (NARX) model with artificial neural network structure, and Nonlinear AutoRegressive Moving Average with eXogenous inputs (NARMAX) models. The best results of each models are compared with respect to precision in free-run simulation. The prediction results show that the most complex NARMAX model had the best results, what encourages further research in creating nonlinear mathematical data-driven abstractions for the piezoacoustic transmission application.

Keywords: Identification and control methods; Smart Structures; Mechatronics; Nonlinear system identification; Artificial Neural Networks; Piezoacoustic Transmission

1. INTRODUCTION

Piezoelectric materials can directly convert an electrical signal into a physical displacement and vice-versa. With those materials it is possible to create smaller and lighter actuators and manage small displacements in the range of sub nanometers to several hundreds of micrometers (Gu et al., 2014). High-precision and high-speed control are a requirement for applications such as micro/nano-positioning and transmission, so an important aspect is modeling and simulation. However, non-linearities such as creep, static and dynamic hytheresis and amplitude, rate and load dependency behaviours, complicate the modelling of piezoelectric actuators. Several first-principles analytical models exists that takes those non-linearities in consideration, such as the Preisach model, Duhem model, Prandtl-Ishlinskii model, Maxwell model, too cite a few (Gu et al., 2014; Rakotondrabe, 2017; Miri et al., 2013). But, due to requirements of physical parameters, computation process complexity, rate dependency, and the necessity of several experiments, to obtain the weight functions and update the model on-line, adaptation to changes of the control conditions degrades (Deng and Tan, 2009; Miri et al., 2013).

One use of piezoelectric actuators is in communication through metal walls. This is interesting in applications were a container or vessel cannot have physical penetrations and due the strong Faraday effect, the use of other through wall techniques such as inductive coupling, capacitive coupling, and magnetic resonance coupling are not feasible (Yang et al., 2015; Shoudy et al., 2007). In this scenario, an active piezoelectric material bounded to the outside wall generates acoustic waves which propagates through the material, also knows as acoustic channel, which may be then recovered by a second piezoelectric material at the inner wall that transduces the received waves for various purposes such as data transmission (Graham et al., 2011), energy harvesting (Hu et al., 2003, 2008) or both (Shoudy et al., 2007; Kluge et al., 2008).

Naturally the physical properties of this channel can severely reduce the efficiency of the transmission and the introduction of multilayered channels, composed of different materials such as steel and water, can pose a challenge to modeling (Takahashi et al., 2019). Although analytical models for this kind of application also exists, the performance suffers from several factors such as roughness of the surfaces, presence of discontinuities in the medium, power losses, and undesired vibrations, to cite a few (Chakraborty et al., 2013; Lawry et al., 2012). As those characteristics are inherent to the system and are challenging to simulate, the models used to tune the control laws should be equipped to better represent the actual system. As such, data-driven modeling such as black-box system identification is a general modeling framework which hinders the difficulties mentioned before. In system identification a black-box model do not require particular knowledge of the physics of the relationship's involved in the system, it is known to have flexibility and can be applied to both linear and non-linear systems (Ljung, 2001). Those properties mitigates the uncertainties of modeling such systems.

Although the use system Identification methodology and data-driven models in Piezoelectric actuators are not new in the literature, such as in Micro/nano-positioning in 1 or 2 degrees of freedom (Ayala et al., 2018, 2015; Cheng et al., 2015), Vibration Control (Dong et al., 2006; Lou et al., 2017), and even in general hysteresis modeling (Deng and Tan, 2009; Yu et al., 2005), there are no works that develops on the challenge of modeling the problem of acoustic transmission of data and power in multiple layers with system identification methodology. That is, the approaches available to identify ultrasonic power and data transfer are still an open issue for the general multilayered case.

In this context, the present work focuses on the application of black-box system identification as a tool for the acoustic transmission modeling problem. The proposed approach is implemented with three data-driven black box models. To identify and estimate the model parameters, a test bench was created to simulate the application scenario and allow data acquisition under designed input signal that covers the whole frequency band of interest. The main objective is to create a model capable that may be used to identify divergences when changes in the medium occurs and calculate the optimal frequency response offline. To this end, we evaluate a swept sine excitation signal and compare the performance of AutoRegressive Moving Average with eXogenous inputs (ARMAX), Nonlinear AutoRegressive Moving Average with eXogenous inputs (NARMAX), and artificial neural networks Nonlinear AutoRegressive with eXogenous inputs (NARX) models for modeling the dynamics of the system using solely input and output data. Being so, the model may be then used for evaluating online the frequency response or to track changes in the system when applied to monitoring.

The present paper is organized as follows. In Section II the case study is presented in details. In Section III the system identification methods employed in the present work are reviewed and in Section IV we give the results of the application of system identification to the problem of acoustic transmission through multiple layers. Lastly, the conclusion and future works are stated in the last Section V.

2. CASE STUDY

The complete test bench can be seen in 1(a). It consists of a signal generator, RF amplifier, oscilloscope and the piezoelectric system.

The acoustic channel of the system studied in this paper consists of two piezoelectric actuators, coupled to one side each of the two steel 5mm thick plates with a layer of epoxy. The two plates are spaced by 100mm and the intermediate region filled with distilled water at room temperature, as show in Fig. 1(b). This creates a system with five layers and three materials (epoxy, steel and water) where both data and energy can be transmitted.

Due to limitations in the hardware available, only the generated input signal (before amplification) and the response output signal (after amplification at receiver) were measured. In this case, the amplifier was made part of the system to be modeled as show in Fig. 2.

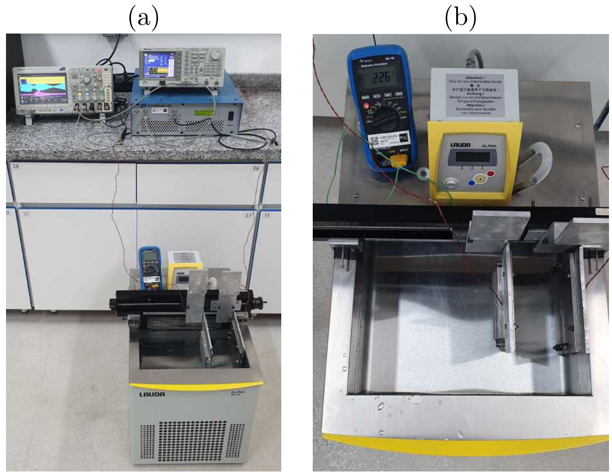

Fig. 1. Picture took from the test bench. (a) Test Bench with amplifier, oscilloscope and signal generator; (b) Steel plates with piezoelectric actuators test bench (on the lower right) at 10 cm away from each other. The tank is filled with distilled water at room temperature.

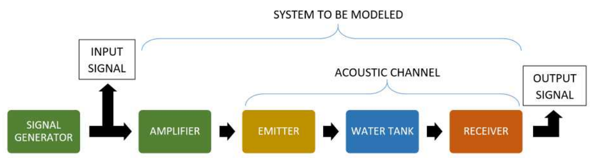

Fig. 2. Schematic drawing of the system showing the input and output acquisition signals location.

2.1 Design of input signals

The choice of input signals is made based on the kind of the experiment under study. They are generated in order to excite the model in several frequency bands, with different amplitudes, and then analyze the system response.

The system was excited using different signal: multisine, square sweep, and linear chirp. Between these three the one chosen to estimate the model was the chirp. This kind of signal excites the system in many frequencies and the rate of change in frequency is a linear function of time. This results in much faster measurement rates and is best suited to making a higher signal-to-noise ratio.

An input chirp signal with amplitude, before amplification, of 80mVpp and 100ms period was generated. The frequency range varied from 900kHz to 1350kHz. This range was chosen because of the specific application and the overall system response is greater at those frequencies.

2.2 Data Pre-Processing

Once the input signal was chosen, the next step was to acquire the data and pre-process it. Pre-processing is an important step of system identification, it leads to better results and also avoids out-of-range values. Since the data of the model is sensitive to noise, this stage is rather relevant.

The acquisition frequency was 100Mhz, resulting in 10 million points for the 100ms period of the signal, which resulted in an over sampled data set. Therefore the first step in the pre-pocessing phase was to resample the data. From Nyquist-Shannon Theorem (Lai, 2003) its possible to measure the minimum-sampling rate at which a continuous-signal can be recovered. But in order to achieve the ideal sampling rate, a method proposed in (Aguirre, 2019) was used as a guideline. This method brought the total number of samples from 10 million to 1 million. In order to further process the resampled data, the frequencies out of the studied range, were removed by a fifth-order band pass filter. From the resampled and filtered data set we used only 2000 samples for creating the models. The reason is that we should limit the number of samples in order to obtain the model predictions for all orders tested. Due to the characteristics of the signal, this sample does not contain the entire frequency range of the original signal.

3. SYSTEM IDENTIFICATION

After the acquisition and pre-processing of the input and output signals from the system, the next step consists of selecting the model structure. The chosen approach is black-box system identification, which builds a mathematical relationship between input and output measured data to reproduce output, without requiring any a priori knowledge about the physical properties of the system. The models are detailed in the sections below.

3.1 ARMAX

In addition to theoretical explanatory variables, the ARMAX model structure includes moving average components and disturbance dynamics, that explain variations in endogenous variables. Its output incorporates previous outputs, inputs, and disturbances. With the moving average error, this structure is useful when dominating disturbances that have entered early in the process (Rachad et al., 2015).

The model can be written as

$$A(q)y(t) = \sum_{i=1}^{n_u} B_i(q)u_i(t - n_{k_i}) + C(q)e(t) \tag{1}$$

where $A(q)$, $B(q)$, and $C(q)$ are polynomials to be estimated. $y(t)$, $u(t)$, and $e(t)$ are respectively output, input, and the residual signals of the system at discrete time t.

The estimation of the ARMAX model parameters requires an iterative method such as prediction errors method (PEM), generalised least squares (GLS), instrumental variables (IV), or extended least squares (Billings, 2013). PEM methods uses numerical optimization to minimize the cost function, a weighted norm of the prediction error. The idea behind this method is to determine the model parameter θ, on 2 such that the residual

$$e(t, \theta) = y(t) - \hat{y}(t|t-1, \theta) \tag{2}$$

is minimized, where $\hat{y}(t|t-1, \theta)$ is the prediction performed using measured data up to $t - 1$. The results for the ARMAX model given in this work used the PEM method for estimating the paramaters of the models.

3.2 NARX

The NARX (Nonlinear AutoRegressive with eXogenous inputs) model is defined as

$$\begin{aligned} y(t) = F[&y(t-1), y(t-2), \ldots, y(t-n_y), \\ &u(t-1), u(t-2), \ldots, u(t-n_u)] + \xi(t); \end{aligned} \tag{3}$$

where n_y and n_u are the maximum lags (or orders of the model) at the output and the input. The function $F[.]$ is in general nonlinear. The residual is defined as

$$\xi(t) = y(t) - \hat{y}(t). \tag{4}$$

The model relates the current value of a time series with its past values and also the exogenous series. It can be efficiently used for modelling non stationary and non linear time series.

The nonlinear functions used for the NARX architecture are the artificial neural network, wavelet network, and a sigmoid network. The neural network approach is a highly parallel distributed network of connected processing units called neurons. These system are able to learn and perform specifics tasks given input and output pairs. The wavelet network consists of a feed-forward neural network with one hidden layer whose activation functions are drawn from an orthonormal wavelet family (Veitch, 2005). The latter follows the same principles of wavelet network, but it uses a sigmoid functions instead.

3.3 NARMAX

The NARMAX (Nonlinear AutoRegressive Moving Average with eXogenous inputs) model is defined as

$$\begin{aligned} y(t) = F[&y(t-1), \ldots, y(t-n_y), \\ &u(t-1), \ldots, u(t-n_u), \\ &e(t-1), \ldots, e(t-n_e)] + e(t) \end{aligned} \tag{5}$$

where $y(t)$, $u(t)$, and $e(t)$ are the system output, input, and residual signals respectively.

The model is a nonlinear difference equation which relates the output of the system at a given time instance to values of the input, outputs, and residual at previous time instance (Unbehauen, 2009). The structure is one of the mostly used for black-box system identification for nonlinear systems. The higher-order polynomials are often selected as the nonlinear function.

The method used for term selection and parameter estimation used on this article was the Forward Regression Orthogonal Least Squares (FROLS) (Billings, 2013). This algorithm uses the principles of the orthogonal least squares (OLS), where the orthogonal function calculates each parameter at a time independently, and the Error Reduction Error (ERR), which is a by product of the OLS algorithm, that shows the significance of each term in the model based on the percentage reduction that each term makes with respect to the output mean squared error (Ahmad and Jamaluddin, 2001). The FROLS uses the basic of the OLS algorithm but at each step of the iteration the best candidate term of the unselected model terms, irrespective of the order, is written down in the model.

3.4 Model Validation

Model validation is the final step of the system identification process. In this step a metric is used to analyze the prediction results of each model and also to validate its consistency. There are several metric to choose to evaluate how well the model fits a set of samples, some are discussed below.

Residuals When building the model, the first metric to review the model quality is the One-Step-Ahead (OSA) residual error. The OSA prediction uses past measured values to calculate the output of the model. Then the residuals can be calculated comparing the predicted value against the measurement. Thus it is possible to evaluate the adherence of the model to the measured data. It is not good practice to analyze the OSA residuals alone and so the Free-run Simulation (FRS) residual error can be used. Instead of using past measured values, the FRS prediction uses past predicted values to calculate the future predictions. Due to its characteristic of using past predictions, it tends to accumulate errors over time, better reflecting the real model capability of representing the system dynamics. In turn, if even OSA residuals are not good, one will not expect good results in FRS. That's why the OSA, despite it's limitations, still a good starting point to first assert the model quality.

Quantitative Metrics Other metrics can be calculated on the basis of the residuals. Those metric offer a more direct comparison between models as those summarize the discrepancy between observed values and the values expected as a single quality number of the estimator. Those are the Mean Squared Error (MSE) and the multiple correlation coefficient (R^2).

The MSE measures the average of the squares of the errors and is always non-negative where values closer to zero are better. The R^2 is not dependent on the amplitude and is a measure of how well a given variable can be predicted. Values closer to one are better. It can be calculated as

$$R^2 = 1 - \frac{\sum_{t=1}^{N} [\xi(t)]^2}{\sum_{t=1}^{N} [y(t) - \bar{y}]^2}. \quad (6)$$

4. RESULTS

In this section we show the results of applying the models based on the ARMAX, NARX and NARMAX to identify the vibro-acoustic system. The output data is given in Fig 3, when the excitation signal is the sine chirp.

In the following sections the best fit of each model is going to be further analysed. At the end of the section, the results for all models analyzed are summarized according to ascending order of R^2 in FRS. The parameters used for the models were defined empirically.

4.1 ARMAX

For this specific model, its parameters n_u, n_y, and n_e orders varied from 1 to 10 generating 1,000 different models. As discussed on section 3.1, its parameters were estimated using the prediction errors method.

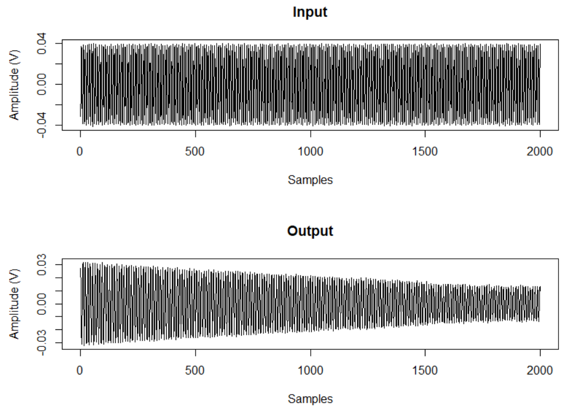

Fig. 3. Input and Output data used for the creation of the model.

The best result obtained using the ARMAX structure was a model with the following orders: $n_y = 10, n_u = 2$,and $n_e = 6$. The model error can be observed on figure 4. Although the model does not include nonlinear terms, the obtained result presented good performance, with $R^2 =$ in FRS.

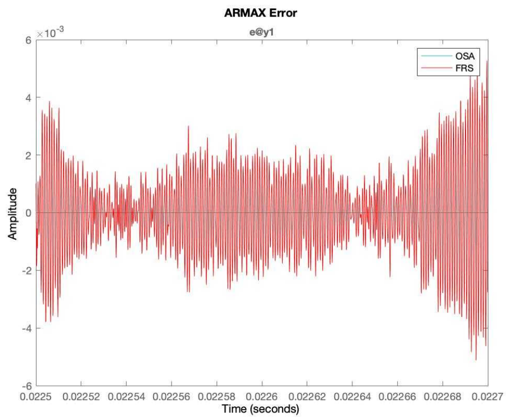

Fig. 4. Error for ARMAX model in OSA (blue) and FRS (red).

4.2 NARX

Both the models orders and its non-linearity estimators where changed in order to achieve better results. n_y and n_u varied from 1 to 20. A higher fit value was obtained with higher total complexity. The model was studied with one or two hidden layers, with a combination of four, five, and ten neurons in each layer. These last were constructed using both a cascade-forward network and feed forward network. A sigmoid and a wavelenet network were also used as non-linearity estimators.

The models that obtained the higher R^2 in FRS used a sigmoid network as the activation function. Compared to the ARMAX error, the NARX error, Fig. 5, is greater on the center part of the samples while the ARMAX error is bigger in the extremities. This may suggests that a ensemble of both models may lead to better fits. The best model in terms of FRS has the following orders: $n_y = 16$, and $n_u = 15$, with $R^2 =$ in FRS.

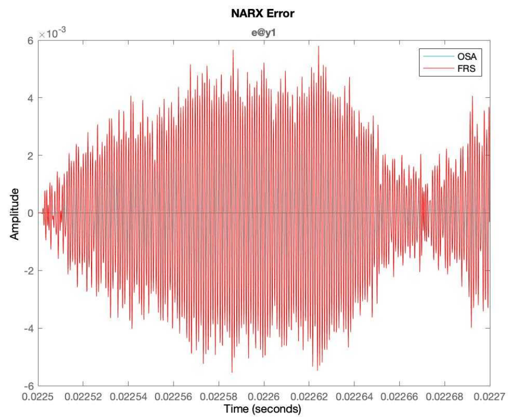

Fig. 5. Error for NARX model in OSA (blue) and FRS (red).

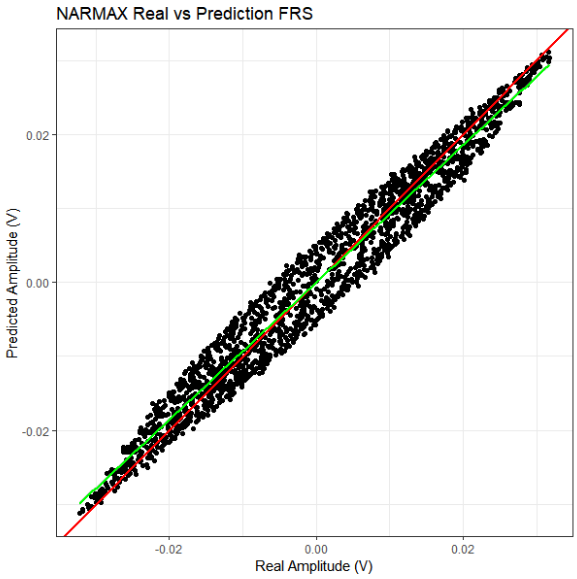

Fig. 6. Measured vs Predicted for the free-run simulation of the best NARMAX model. In red the $y = x$ curve and in green the fitted linear regression for the predictions.

4.3 NARMAX

In order to construct the NARMAX models, we tested all possible combinations for the parameters n_u, n_y and n_e in the range [1,10]. The non-linearity tested was $n_l = 2$. For all model orders, we tested the threshold ρ_p in the range $[10^{-4}, 10^{-5}]$, always having $\rho_n = 10^{-1}\rho_p$.

The best result obtained using the NARMAX structure was a model with the following parameters: $n_u = 1, n_y = 2, n_e = 3$, $n_l = 2$, $\rho_p = 10^{-6}$, and $\rho_n = 10^{-7}$. As shown in Fig. 6 and Fig. 7 the model has reasonable accuracy for prediction. The scatterplot of the predictions vs. the measurements is close to the line with 45° slope which represent the ideal model prediction.

4.4 Summary of all models tested

In Table 1 we show a description of the best models for each class tested, in terms of R^2 in FRS. We can see that higher complexity obtained overall better results.

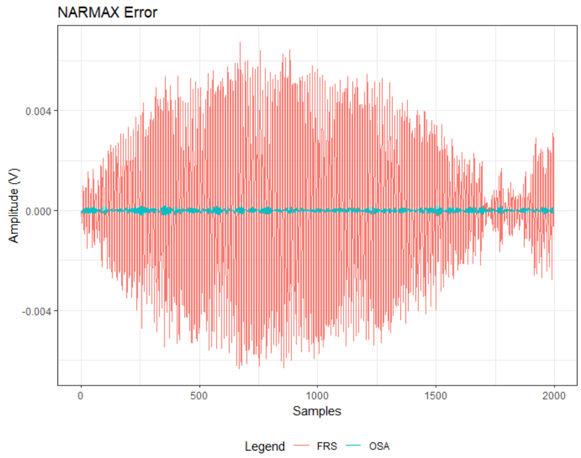

Fig. 7. Error for NARMAX model in OSA (blue) and FRS (red)

Table 1. All models ordered by ascending order of R^2 in FRS.

model	n_u	n_y	n_e	n_l	ρ_p	ρ_n	R2 FRS
3	19	17	NA	NA	NA	NA	0.8830
3	17	16	NA	NA	NA	NA	0.8830
3	18	18	NA	NA	NA	NA	0.8880
3	15	16	NA	NA	NA	NA	0.8920
2	1	5	2	1	NA	NA	0.9000
2	1	5	5	1	NA	NA	0.9010
2	2	10	7	1	NA	NA	0.9040
2	1	8	3	1	NA	NA	0.9040
2	2	10	6	1	NA	NA	0.9060
1	1	3	1	2	10^{-4}	10^{-5}	0.9396
1	1	2	8	2	10^{-4}	10^{-5}	0.9612
1	1	2	3	2	10^{-4}	10^{-5}	0.9629
1	1	2	3	2	10^{-6}	10^{-7}	0.9651
1	4	5	10	2	10^{-6}	10^{-7}	0.9815
1	4	4	1	2	10^{-6}	10^{-7}	0.9819
1	4	6	4	2	10^{-6}	10^{-7}	0.9822
1	4	5	8	2	10^{-6}	10^{-7}	0.9824

In this table, NARMAX (1), had the best results, with a greater margin, when compared to the ARMAX (2) and NARX(3). It is possible to see that the predictions are close to unity in FRS for the NARMAX case, what confirms this model ability to represent the dynamics of the system using measured data.

5. CONCLUSION

The present work demonstrated the identification of the acoustic transmission system through multiple layers with piezoelectric actuators using black-box models. We have successfully applied several models, namely the linear ARMAX, NARX with artificial neural networks model structure and the power-form polynomial NARMAX models, and compared them with real-world acquired data. The proposed models are an alternative to analytical model, when computational performance is important for monitoring as environmental changes may take place. The model is thus useful for tracking time-varying systems that is relevant for such application, as their frequency response determines the maximum gain and is influenced by the parameters of the obtained model.

Future research will be devoted to construct models with general purpose signals such as the random phase multisine and model validation with exclusive datasets. It will also be sought to study how different assumptions of changes in the operational conditions affects the model performance, such as the distance between the plates, and fluid temperature and type. As the bandwidth and sampling frequency required by the system are large, we also think that new methods for handling big datasets are handful for black-box modeling in this application.

REFERENCES

Aguirre, L.A. (2019). A Bird's Eye View of Nonlinear System Identification. *arXiv e-prints*, arXiv:1907.06803.

Ahmad, R. and Jamaluddin, H. (2001). Orthogonal least square algorithm and its application for modelling suspension system. *Jurnal Teknologi*, 34(1), 71–84.

Ayala, H.V.H., Habineza, D., Rakotondrabe, M., Klein, C.E., and Coelho, L.S. (2015). Nonlinear black-box system identification through neural networks of a hysteretic piezoelectric robotic micromanipulator. *IFAC-PapersOnLine*, 48(28), 409–414.

Ayala, H.V.H., Rakotondrahe, M., and dos Santos Coelho, L. (2018). Modeling of a 2-dof piezoelectric micromanipulator at high frequency rates through nonlinear black-box system identification. In *2018 Annual American Control Conference (ACC)*, 4354–4359. IEEE.

Billings, S.A. (2013). *Nonlinear system identification: NARMAX methods in the time, frequency, and spatio-temporal domains.* John Wiley & Sons.

Chakraborty, S., Wilt, K.R., Saulnier, G.J., Scarton, H.A., and Das, P.K. (2013). Estimating channel capacity and power transfer efficiency of a multi-layer acoustic-electric channel. In *Wireless Sensing, Localization, and Processing VIII*, volume 8753, 87530F. International Society for Optics and Photonics.

Cheng, L., Liu, W., Hou, Z.G., Yu, J., and Tan, M. (2015). Neural-network-based nonlinear model predictive control for piezoelectric actuators. *IEEE Transactions on Industrial Electronics*, 62(12), 7717–7727.

Deng, L. and Tan, Y. (2009). Modeling hysteresis in piezoelectric actuators using narmax models. *Sensors and Actuators A: Physical*, 149(1), 106–112.

Dong, X.J., Meng, G., and Peng, J.C. (2006). Vibration control of piezoelectric smart structures based on system identification technique: Numerical simulation and experimental study. *Journal of sound and vibration*, 297(3-5), 680–693.

Graham, D.J., Neasham, J.A., and Sharif, B.S. (2011). Investigation of methods for data communication and power delivery through metals. *IEEE Transactions on industrial electronics*, 58(10), 4972–4980.

Gu, G.Y., Zhu, L.M., Su, C.Y., Ding, H., and Fatikow, S. (2014). Modeling and control of piezo-actuated nanopositioning stages: A survey. *IEEE Transactions on Automation Science and Engineering*, 13(1), 313–332.

Hu, H., Hu, Y., Chen, C., and Wang, J. (2008). A system of two piezoelectric transducers and a storage circuit for wireless energy transmission through a thin metal wall. *IEEE transactions on ultrasonics, ferroelectrics, and frequency control*, 55(10), 2312–2319.

Hu, Y., Zhang, X., Yang, J., and Jiang, Q. (2003). Transmitting electric energy through a metal wall by acoustic waves using piezoelectric transducers. *IEEE Transactions on Ultrasonics, Ferroelectrics, and Frequency Control*, 50(7), 773–781.

Kluge, M., Becker, T., Schalk, J., and Otterpohl, T. (2008). Remote acoustic powering and data transmission for sensors inside of conductive envelopes. In *SENSORS, 2008 IEEE*, 41–44. IEEE.

Lai, E. (2003). 2 - converting analog to digital signals and vice versa. In E. Lai (ed.), *Practical Digital Signal Processing*, 14 – 49. Newnes, Oxford.

Lawry, T.J., Wilt, K.R., Scarton, H.A., and Saulnier, G.J. (2012). Analytical modeling of a sandwiched plate piezoelectric transformer-based acoustic-electric transmission channel. *IEEE transactions on ultrasonics, ferroelectrics, and frequency control*, 59(11), 2476–2486.

Ljung, L. (2001). Black-box models from input-output measurements. In *IMTC 2001. Proceedings of the 18th IEEE instrumentation and measurement technology conference. Rediscovering measurement in the age of informatics (Cat. No. 01CH 37188)*, volume 1, 138–146. IEEE.

Lou, J., Liao, J., Wei, Y., Yang, Y., and Li, G. (2017). Experimental identification and vibration control of a piezoelectric flexible manipulator using optimal multi-poles placement control. *Applied Sciences*, 7(3), 309.

Miri, N., Mohammadzaheri, M., and Chen, L. (2013). A comparative study of different physics-based approaches to modelling of piezoelectric actuators. In *2013 IEEE/ASME International Conference on Advanced Intelligent Mechatronics*, 1211–1216. IEEE.

Rachad, S., Nsiri, B., and Bensassi, B. (2015). System identification of inventory system using arx and armax models.

Rakotondrabe, M. (2017). Multivariable classical prandtl–ishlinskii hysteresis modeling and compensation and sensorless control of a nonlinear 2-dof piezoactuator. *Nonlinear Dynamics*, 89(1), 481–499.

Shoudy, D., Saulnier, G., Scarton, H., Das, P., Roa-Prada, S., Ashdown, J., and Gavens, A. (2007). P3f-5 an ultrasonic through-wall communication system with power harvesting. In *2007 IEEE Ultrasonics Symposium Proceedings*, 1848–1853. IEEE.

Takahashi, V.L., Kubrusly, A.C., Braga, A., Quintero, S.M., Figueiredo, S.W., and Domingues, A.B. (2019). Ultrasonic power and data transfer through multiple curved layers applied to pipe instrumentation. *Sensors*, 19(19), 4074.

Unbehauen, H.D. (2009). *CONTROL SYSTEMS, ROBOTICS AND AUTOMATION–Volume VI: Modeling and System Identification-III.* EOLSS Publications.

Veitch, D. (2005). Wavelet neural networks. *Produced by University of UK.*

Yang, D.X., Hu, Z., Zhao, H., Hu, H.F., Sun, Y.Z., and Hou, B.J. (2015). Through-metal-wall power delivery and data transmission for enclosed sensors: A review. *Sensors*, 15(12), 31581–31605.

Yu, S., Alici, G., Shirinzadeh, B., and Smith, J. (2005). Sliding mode control of a piezoelectric actuator with neural network compensating rate-dependent hysteresis. In *Proceedings of the 2005 IEEE International Conference on Robotics and Automation*, 3641–3645. IEEE.